Received: 30 May 2023 | Revised: 22 October 2023 | Accepted: 10 November 2023

DOI: 10.1111/odi.14816

ORAL DISEASES Leading in Oral, Maxillofacial, Head & Neck Medicine WILEY

ORIGINAL ARTICLE

Whole genome sequencing in families with oligodontia

Janna Mitscherling[1] | Henrike L. Sczakiel[2,3,4] | Olga Kiskemper-Nestorjuk[1] | Sibylle Winterhalter[5] | Stefan Mundlos[2,4] | Theodosia Bartzela[1,6] | Martin A. Mensah[2,4,7]

[1]Department of Orthodontics and Dentofacial Orthopedics, Charité – Centrum 03 für Zahn-, Mund- und Kieferheilkunde, Charité – Universitätsmedizin Berlin, Freie Universität Berlin, Humboldt-Universität zu Berlin, und Berlin Institute of Health, Berlin, Germany

[2]Institute of Medical Genetics and Human Genetics, Charité – Universitätsmedizin Berlin, Freie Universität Berlin and Humboldt-Universität zu Berlin, Berlin, Germany

[3]BIH Biomedical Innovation Academy, Junior Clinician Scientist Program, Berlin Institute of Health at Charité – Universitätsmedizin Berlin, Berlin, Germany

[4]RG Development & Disease, Max Planck Institute for Molecular Genetics, Berlin, Germany

[5]Department of Ophthalmology, Charité – Universitätsmedizin Berlin, Freie Universität Berlin and Humboldt-Universität zu Berlin, Berlin, Germany

[6]Department of Orthodontics, Technische Universität Dresden, Dresden, Germany

[7]BIH Biomedical Innovation Academy, Digital Clinician Scientist Program, Berlin Institute of Health at Charité – Universitätsmedizin Berlin, Berlin, Germany

Correspondence
Martin A. Mensah, Institute of Medical Genetics and Human Genetics, Charité – Universitätsmedizin Berlin, Freie Universität Berlin and Humboldt-Universität zu Berlin, Augustenburger Platz 1, Berlin 13353, Germany.
Email: martin-atta.mensah@charite.de

Abstract

Background/Objectives: Tooth agenesis (TA) is among the most common malformations in humans. Although several causative mutations have been described, the genetic cause often remains elusive. Here, we test whether whole genome sequencing (WGS) could bridge this diagnostic gap.

Methods: In four families with TA, we assessed the dental phenotype using the Tooth Agenesis Code after intraoral examination and radiographic and photographic documentation. We performed WGS of index patients and subsequent segregation analysis.

Results: We identified two variants of uncertain significance (a potential splice variant in *PTH1R*, and a 2.1 kb deletion abrogating a non-coding element in *FGF7*) and three pathogenic variants: a novel frameshift in the final exon of *PITX2*, a novel deletion in *PAX9*, and a known nonsense variant in *WNT10A*. Notably, the *FGF7* variant was found in the patient, also featuring the *WNT10A* variant. While mutations in *PITX2* are known to cause Axenfeld-Rieger syndrome 1 (ARS1) predominantly featuring ocular findings, accompanied by dental malformations, we found the *PITX2* frameshift in a family with predominantly dental and varying ocular findings.

Conclusion: Severe TA predicts a genetic cause identifiable by WGS. Final exon *PITX2* frameshifts can cause a predominantly dental form of ARS1.

KEYWORDS
genetics, genomics, growth/development, molecular genetics, oligodontia, tooth development

Janna Mitscherling and Henrike L. Sczakiel contributed equally.

Theodosia Bartzela and Martin A. Mensah shared last authorship.

1 | INTRODUCTION

1.1 | Background

Next-generation sequencing (NGS) has revolutionized genetic testing. However, due to a lack of knowledge about the functional impact of many genetic variants on organ development, it has not yet reached its full potential as a diagnostic tool in congenital malformation syndromes. (Elsner et al., 2021).

The dentition is an eminently suitable object for studying the genetic basis of the development of organs and possible disturbances thereof. Teeth are readily accessible to clinical examination, congenital dental malformations are relatively frequent, the denture is composed of different tissues and its embryonic differentiation governed by the same signaling pathways controlling the formation of numerous other organs. (Bailleul-Forestier et al., 2008; de La Dure-Molla et al., 2019).

The dental anlagen of both the deciduous and permanent set of teeth are prenatally formed. Specific mesenchymal cells in the embryonic oral cavity derived from neural crest cells induce the formation of teeth (odontogenesis) in the ectodermal cells above. The ectodermal cells bulge out into the underlying mesenchyme and teeth are formed by an interplay of both tissue types, governed by BMP, FGF, and WNT/SHH signaling (Figure 1). Eventually, the enamel is a derivative of the ectoderm, and the remaining parts of a tooth have a mesenchymal origin. During postnatal growth, the germs of the permanent teeth mature and eventually displace the deciduous teeth that lie above them. (Bilodeau & Hunter, 2021; Thesleff, 2014).

Inborn malformations of the denture often concern a reduced number of permanent teeth detectable upon visual inspection. Two forms of inheritably missing teeth can be defined: failure of a tooth to develop prenatally (tooth agenesis, TA) and failure to emerge to the oral cavity postnatally (primary failure of eruption, PFE). While in PFE teeth can be radiographically detected in the adult jaw, they are genuinely absent in TA (Bailleul-Forestier et al., 2008).

Depending on the number of teeth absent from the permanent dentition (not counting third molars), three types of TA are distinguished: Hypodontia with up to five missing teeth, oligodontia with six or more missing teeth, and anodontia featuring the absence of all permanent teeth (Al-Ani et al., 2017). TA is considered one of the most frequent congenital dentofacial malformations in humans (Matalova et al., 2008). The exact prevalence, however, is hard to estimate and reports vary from 1.6% to values as high as 36.5% depending on the studied population (Al-Ani et al., 2017; Murakami et al., 2017). PFE and TA may occur as isolated traits or as parts of genetic syndromes (i.e., accompanied by other malformations) (Cobourne & Sharpe, 2013).

Especially the investigation of genetic causes of PFE and TA has been challenging. Nevertheless, the advent of high-throughput

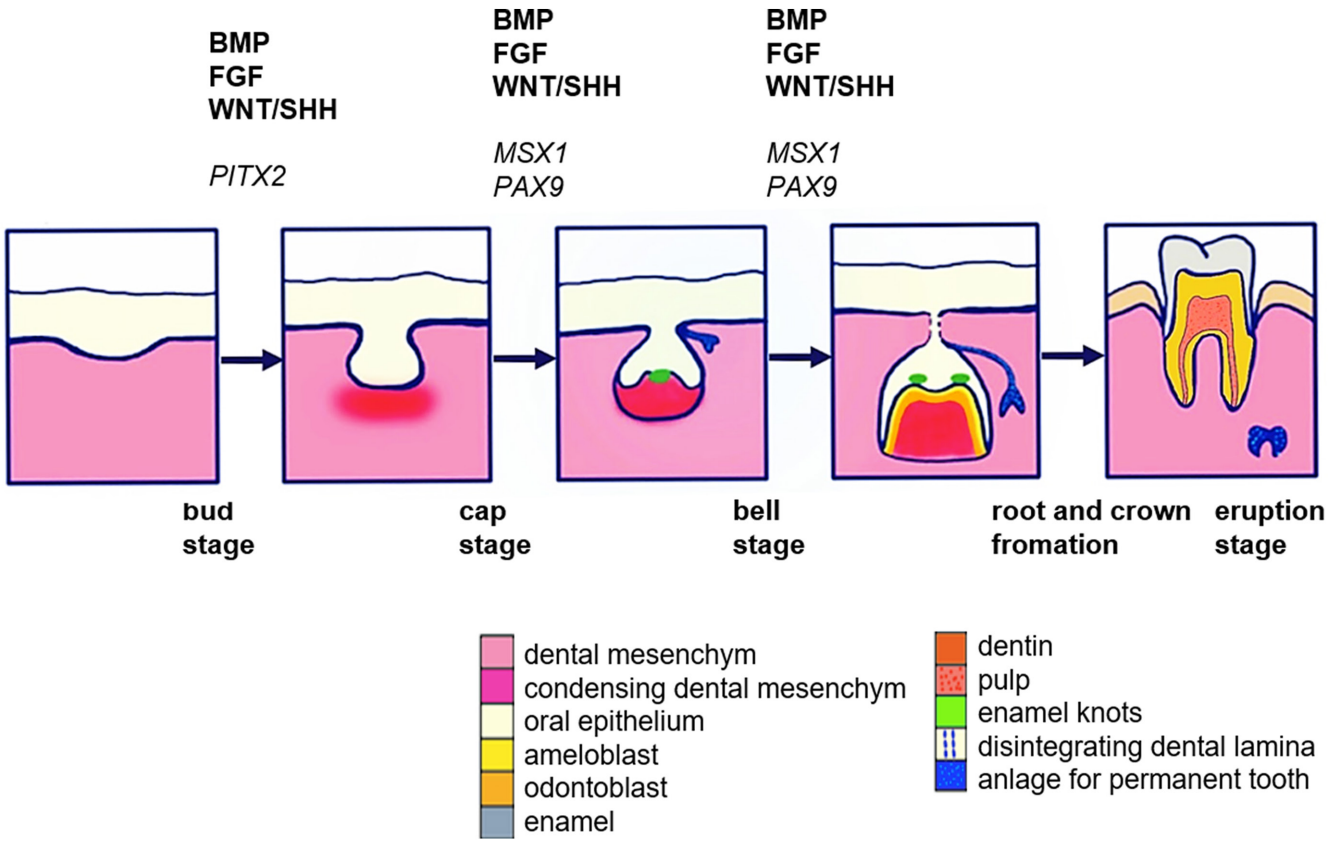

FIGURE 1 Schematic representation of the embryonic tooth development and involved pathways.

sequencing has resulted in an unprecedented boost of genetic studies, and mutations in numerous genes have been linked to a reduced number of teeth since (in e.g., *PTH1R* (Decker et al., 2008), *MSX1* (Zheng et al., 2021), *AXIN2* (Wong et al., 2014), *EDA* (Song et al., 2009; Stockton et al., 2000), *EDAR* (Song et al., 2009), *EDARADD* (Song et al., 2009), *PAX9* (Song et al., 2009), *WNT10A* (Arte et al., 2013), and *LRP6* (Massink et al., 2015)). Yet, relevant genetic alterations could not be identified in all affected families (Biedziak et al., 2022; Williams & Letra, 2018) and the role of non-coding variants remains largely unknown. This hampers targeted genetic sequencing for diagnostic purposes in patients with tooth agenesis.

NGS and in particular whole genome sequencing (WGS) facilitate the unconstrained testing of an individual's almost complete genetic information (Biedziak et al., 2022; Turro et al., 2020). This could aid in identifying pathogenic variants in known tooth agenesis genes and in estimating the functional and clinical relevance of non-coding variants. The identification of new variants and genes associated with the phenotype could broaden the understanding of the development of teeth and ultimately of organogenesis in general.

1.2 | Objective

Studies using WGS on patients with dental malformations, particularly on patients with oligodontia, are, thus, needed (Biedziak et al., 2022; Williams & Letra, 2018).

We aimed to test the potential use of WGS in the diagnostic workup of patients with oligodontia. We also sought to identify new pathogenic mutations as well as novel candidate genes causing oligodontia.

2 | MATERIALS AND METHODS

2.1 | Patient inclusion

To be eligible for genome sequencing, patients had to feature a suggestive diagnosis of oligodontia, that is, missing of at least six permanent teeth (not regarding third molars). The minimum age of the included participants was 9 years, in order to exclude patients with a delayed dental development.

In total, 11 individuals from four families were included.

2.2 | Patient selection

Patients featuring a reduced number of teeth were recruited from the Department of Orthodontics and Dentofacial Orthopedics of the Charité—Universitätsmedizin Berlin. To be eligible for inclusion patients had to feature a suggestive clinical diagnosis of PFE or oligodontia and no prior genetic test. Patients and their family members were included after they or their legal guardians gave written informed consent in accordance with the Declaration of Helsinki and the terms of the ethical review board of the Charité—Universitätsmedizin Berlin.

2.3 | Dental evaluation

Dental parameters of index patients (and both parents, if available) were assessed and described using the Tooth Agenesis Code (TAC) (van Wijk & Tan, 2006). Individual orodental findings were documented by intraoral photographs and panoramic radiographs using a Canon EOS 100D camera and a Sirona Orthophos XG 3D system, respectively.

A dentist determined the number of missing, existing, and extracted teeth by intraoral examination and evaluation of patient records. A second dentist independently reassessed all available records, intraoral clinical photographs, and radiographic images. If the ratings did not match, images were reviewed, and a consensus was reached.

2.4 | Ophthalmologic evaluation

Ophthalmologic examination of the anterior and posterior segment was performed by an ophthalmologist using a Haag Streit slit lamp. Intraocular pressure was taken by Goldmann tonometry and gonioscopy was performed with a Haag Streit Goldmann three mirror contact glass 903 L.

Optic nerve head and macular measurements were performed using Spectral Domain Optical Coherence Tomography (SD-OCT) (Heidelberg Eye Explorer version 6.9a, Heidelberg Spectralis, Heidelberg Engineering, Heidelberg, Germany).

The G top strategy of the Octopus 900 Haag Streit international perimeter was used for visual field examination.

2.5 | Evaluation of other clinical findings

Patients' general medical histories were taken from clinical reports of their general practitioners and pediatricians, respectively.

2.6 | Genetic testing

2.6.1 | Sample preparation and whole genome sequencing

DNA was extracted from blood lymphocytes using standard protocols. PCR-free, Illumina paired-end, 150 bp short read whole genome sequencing of index DNA samples was performed. FASTQ files were processed by the Core Unit Bioinformatics of the Berlin Institute of Health (CUBI) as described previously (Elsner et al., 2021).

2.6.2 | Variant filtration

In particular, variants were filtered using the system for Omics Data Analysis and Retrieval v.2 (SODAR Beta) (Nieminen et al., 2020) and the VarFish (Holtgrewe et al., 2020) Ballonaster (vv1.2.0) platform as described previously. Small variants were filtered by sequencing quality (coverage ≥ 10× for heterozygous and ≥5× for homozygous variants, allelic balance ≥ 0.2, reads showing variant ≥ 3), minor allele frequency (0.01 and maximum of 0 homozygous counts in gnomAD exomes, gnomAD genomes, 1000 Genomes and ExAC databases for heterozygous variant filtration; 0.01 and maximum of 20 homozygous counts in gnomAD exomes, 4 in gnomAD genomes, 4 in 1000 Genomes, and 10 in ExAC databases, as well as 1200 heterozygous counts in gnomAD exomes, 150 in gnomAD genomes, 240 in 1000 Genomes, and 600 in ExAC for homozygous variant filtration), and variant localization (exomic +/−20 bp). Using these filter settings, variants were further filtered more strictly, according to variant impact (coding or splice site variants), assuming different modes of inheritance and prioritized by predicted pathogenicity (CADD score (Rentzsch et al., 2021)) and phenotypic match. "HP:0000677 - Oligodontia" was used as the HPO term for variant prioritization by phenotype. Of note, the phenotype score calculated by VarFish takes into account all gene–phenotype relations listed in the Online Mendelian Inheritance in Men (OMIM; https://www.omim.org/) as well as all published, PubMed listed data on the respective gene. Structural variants (≥50 bp) were filtered by sequencing quality (coverage ≥4, reads covering variant ≥3, split read supporting variant ≥1, read pair supporting variant ≥1, allelic balance ≥0.2), and minor allele frequencies (maximum variant carriers: 20 in DGV, 10 in DGV Gold Standard, 40 in dbVar, 20 in ExAC, 10 in 1000 Genomes, 20 in gnomAD SVs, 5 in inhouse database). A schematic workflow of filter steps can be found in Figure S3.

2.6.3 | Variant confirmation

Potentially pathogenic variants were confirmed and segregated either by targeted Sanger sequencing (small variants), breakpoint PCR, and Sanger sequencing (deletions ≥ 50 bp) or quantitative PCR (deletions ≥ 50 bp) using standard protocols. The following primers were used to amplify the respective fragments from genomic DNA: PTH1R_F: AGGACGCTGTGCTCTACTCTG, PTH1R_R: ACGGGTTTGAGTGGCTGA; FGF7_Del_F: GCATCAAGGAACCCAACGGAA, FGF7_Del_R: GGGTTTCCTAGGCTAGAGGTTG; WNT10A_Ex2_F: AGGGAGTGATTATGGCCGTTG, WNT10A_Ex2_R: CCAGGAGTCCAGTTCTAAGGC; PITX2_F: TATGAACGTCAACCCCCTGT, PITX2_R: GGCCAGGCTCGAGTTACAC; PAX9_5'_F: CCACTTTACTTGGCCGTAGG, PAX9_5'_R: GTCCCTGAACATAGCCGAAC, PAX9_Del-1_F: ACACATCCGGACCTACAAGC, PAX9_Del-1_R: ACGGAGGGCACATTGTACTT, PAX9_Del-2_F: TCCATCACCGACCAAGGTA, PAX9_Del-2_R: GGGAAAGACAGTGTCCCTGA, PAX9_3'_F: CCCTGTTCATGGGAAAGTGT, PAX9_3'_R: TGGGCACAAGCTTGAAGTTA.

2.6.4 | Variant classification

Reported variants were classified according to current ACMG guidelines, the de facto global standard for variant classification (Richards et al., 2015; Riggs et al., 2020). The ACMG uses a 5-tier classification scheme reaching from benign (class I) to pathogenic (class V). Variants are scored according to their population frequency, computational information, functional impact, segregation, and database information using structured criteria of seven levels (strong and supporting benign, as well as supporting, moderate, strong, and very strong pathogenic). Evolutionary conservation was visualized using MutationTaster (Schwarz et al., 2014) and the UCSC genome browser (Kent et al., 2002). Pathogenicity rating and splice prediction were performed using CADD score (Rentzsch et al., 2021), MutationTaster (Schwarz et al., 2014), REVEL (Ioannidis et al., 2016) and SpliceAI (Jaganathan et al., 2019). Non-coding variants were evaluated with respect to their sequence conservation, histone modification (Histone 3 lysine 27 acetylation (H3K27Ac), histone 3 lysine 4 monomethylation (H3K4Me1) and histone 3 lysine 4 trimethylation (H3K4Me3)) and prediction of candidate cis-regulatory elements (cCREs) according to the ENCODE project consortium (ENCODE Project Consortium et al., 2020) and prediction of enhancers and promotors from the GeneHancer database (Fishilevich et al., 2017).

2.7 | Bibliographic search

PubMed was searched using the search string "(Oligodontia OR hypodontia OR 'tooth agenesis' OR 'missing teeth') AND (PAX9 OR PTH1R)" in September 2022. The abstracts of yielded articles were screened manually for relevance and articles were eventually included if they provided a comprehensive description of the dental phenotype (i.e., if they presented an orthopantomogram or textual or tabular description of the complete dental status).

Also, the Human Gene Mutation Database (HGMD, https://apps.ingenuity.com/ingsso/login) (Stenson et al., 2014) was searched to explore *PITX2*- and *PAX9*-associated cases published to date. All papers deposited in HGMD on *PITX2* and *PAX9*, respectively, were examined. Cases were included in the cohort of published cases presented here if detailed dental findings (OPTG and/or TAC code) were available.

2.8 | Ethic vote

This study has been approved by the ethical review board of the Charité – Universitätsmedizin Berlin (ethical vote: EA2/197/20) and was conducted in accordance with the Declaration of Helsinki.

Written informed consent was obtained from all participants or their legal guardians.

3 | RESULTS

3.1 | Phenotypes of included individuals

Eleven individuals of four families matched the inclusion criteria and were eligible for genetic testing. To prepare genetic analysis, index patients and relevant available family members were clinically phenotyped.

3.1.1 | Family 1

Individual 1 is a 16-year-old female of German descent with a height of 168 cm and a weight of 80 kg. Her general medical and family history were unremarkable. The dental history was unremarkable in the primary dentition. In the permanent dentition, however, agenesis of eight teeth (15, 14, 12, 22, 24, 25, 37, 35) was registered (missing third molars not counted) (Figure 2a–c).

In this case, only the 58-year-old mother featuring a normal dentition and unremarkable general medical history was available for further evaluation. The father was reported to have a complete set of teeth. (Figure 2d).

3.1.2 | Family 2

Individual 2 is a 22-year-old male of German descent with a height of 186 cm and a weight of 80 kg. His general medical history was unremarkable. No missing teeth in the primary dentition were reported. In the permanent dentition a total of 10 teeth (17, 13, 12, 22, 23, 37, 35, 31, 45, 47) were missing (not counting third molars) (Figure 3a–c). Notably, four deciduous teeth (53, 62, 63, 85) severely affected by caries persisted.

Both parents were available for testing and examination. The 53-year-old mother featured an unremarkable general medical history. She had no congenitally missing teeth. Also, the 59-year-old father had no congenitally missing teeth (Figure 3d). He had been diagnosed with osteosarcoma of the right femur at the age of 55.

3.1.3 | Family 3

Individual 3 is a 17-year-old female with a height of 172 cm, a weight of 54 kg and an occipitofrontal head circumference (OFC) of 55.5 cm. Her dental history was unremarkable in the primary dentition. In the permanent dentition, a total of 11 teeth (16, 13, 12,11, 22, 23, 26, 37, 31, 41, 47) were missing. She had the following persistent deciduous teeth 55, 53, 63, 65, 75, 81 and a microdont 21 (Figure 4a,b,d). Her ophthalmologic history showed a posterior embryotoxon of the right eye and a corectopia of the left eye with multiple peripheral anterior adhesions, but normal intraocular pressures and optic nerve heads in both eyes (Figure 4c). Additionally, she had a tonsillotomy at the age of 4 years.

Her 41-year-old father of Russian and German descent featured a height of 184 cm, a weight of 84 kg, and an OFC of 57.5 cm. He gave an unremarkable general medical history. He featured oligodontia with 12 teeth (14, 12, 22, 24, 27, 37, 33, 32, 31, 41, 43, 45) missing from the permanent dentition (not counting third molars) (Figure 4h; Figure S1a,b). According to the father's report, the teeth were missing congenitally, and his mother and maternal grandfather suffered from missing teeth and poor vision. (Figure 4e).

The 40-year-old mother of individual 3 presented with an inconspicuous general medical history and no congenitally missing teeth.

3.1.4 | Family 4

Individual 4 is a 16-year-old female of German descent with a height of 165 cm and a weight of 60 kg. Her general medical history and family history were unremarkable. Agenesis of eight permanent teeth (17, 16, 15, 12, 25, 26, 27, 31, third molars not counted) was registered. The primary dentition was unremarkable and two deciduous teeth were persistent (53, 71) (Figure 5a–c).

3.2 | Results of whole genome sequencing

To identify possible causative genetic variants, index patients were sequenced by WGS and data were filtered for rare, potentially harmful variants. All parents that were available for genetic testing were subjected to segregation analysis of variants of interest by targeted Sanger sequencing, quantitative PCR, or breakpoint PCR (Figure S2).

3.2.1 | Family 1

Of the 3,026,114 variants called in individual 1 only 26 were of good quality, exomic, affecting the predicted amino acid sequence, rare, and predicted to be phenotypically relevant (Figure 2f). Of these only the variant *PTH1R*(NM_000316.3):c.834+11C>A p.? could be linked to a reduced number of teeth. *PTH1R* encodes the parathyroid hormone receptor 1 and heterozygous pathogenic loss-of-function variants of *PTH1R* are associated with primary failure of tooth eruption (Decker et al., 2008). Segregation analysis showed that the individual's mother is not a carrier of this *PTH1R* variant. The individual's father was not available for genetic testing (Figure 2d; Figure S2a–c).

3.2.2 | Family 2

In individual 2 phenotypic prioritization of whole genome variant calls directly suggested the heterozygous nonsense variant

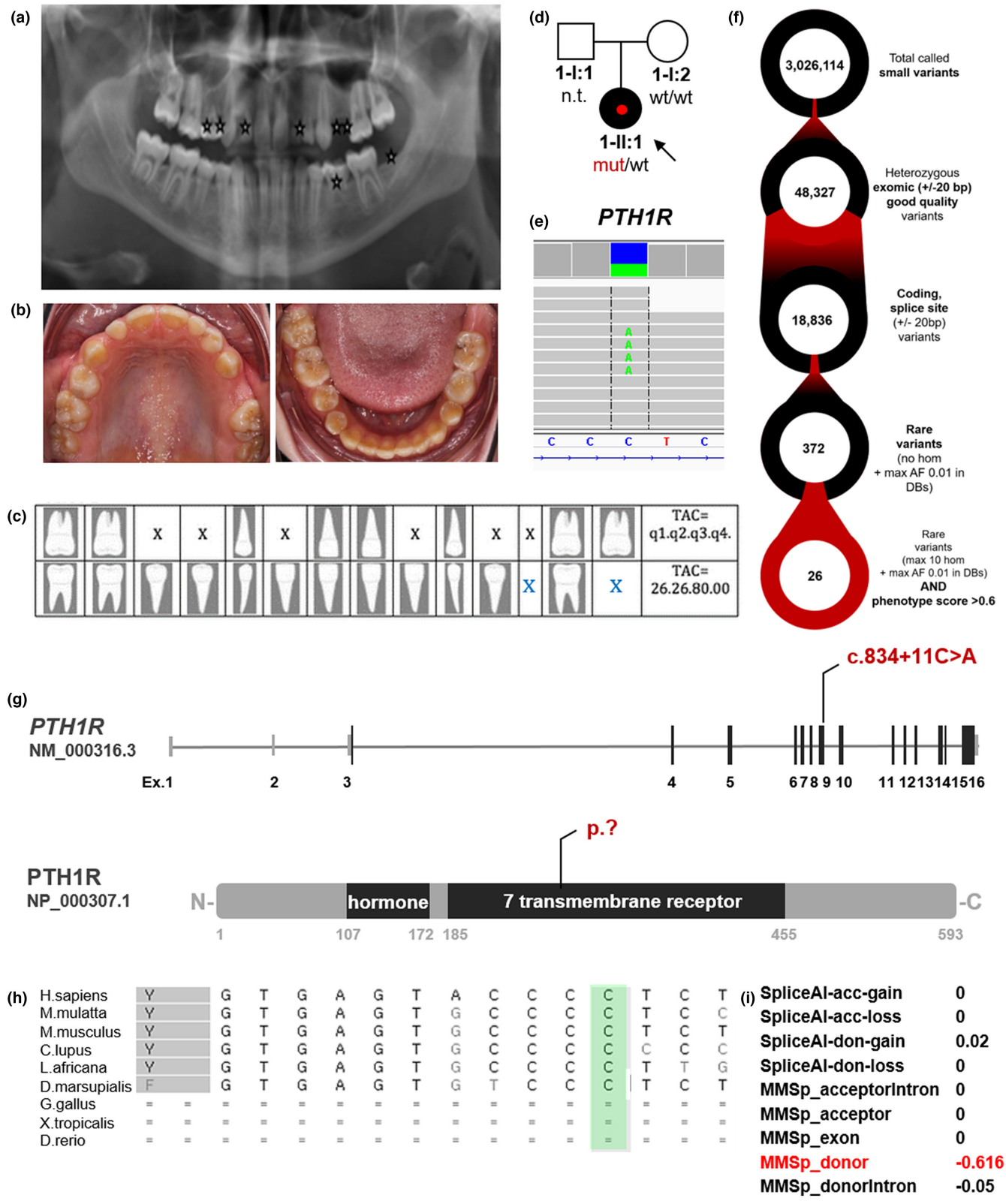

FIGURE 2 Clinical and molecular findings in individual 1: (a) Orthopantomogram shows missing teeth (*) 15, 14, 12, 22, 24, 25, 37, 35. (b) Intraoral photographs of the index patient's maxilla and mandible show missing teeth 15, 14, 12, 22, 24, 25, 37, 35, persistent deciduous teeth 52, 54, 62, 63, 75, 85. (c) Schematic representation of the missing teeth and coding of the phenotype with the TAC code. Asymmetric missing teeth are indicated by the blue X. (d) pedigree: affected individuals are shown in black, mutation carriers are marked by a red dot, arrow: index, mut: mutant allele, wt: wildtype allele, n.t.: not tested. (e) IGV screenshot of the index' NGS data showing the identified *PTH1R* variant in heterozygous state. (f) Genome SNV filter strategy leading to the identified *PTH1R* variant. (g) *PTH1R* gene (above) and protein (below). Exons (Ex.) 1–16 (above, gene), functional domains (protein, below), and the location of the identified variant within these are depicted. (h) Conservation of the affected position (highlighted in green) on genomic DNA across different species. (i) Splice effect predictions retrieved from SpliceAI and MMSp.

WNT10A(NM_025216.3): c.321C>A p.(Cys107*). Intriguingly, both mono- and biallelic *WNT10A* variants are known to cause oligodontia (Adaimy et al., 2007; Arte et al., 2013; Bohring et al., 2009; Yu et al., 2019). Notably, segregation analysis revealed inheritance of the *WNT10A* variant from the unaffected mother (Figure 3d; Figure S2d–f).

We, thus, hypothesized that the mode of inheritance could actually be di- or oligogenic with other loci determining the penetrance of single pathogenic *WNT10A*-variants.

Sequencing data were, therefore, further filtered for potential causative variants. No potentially relevant SNV could be identified. Of the 20,986 called structural variants, 933 were larger than 50 bp and of good quality including 184 rare variants. No exomic structural variants were identified. However, structural variant calls comprised a deletion of 2116 bp on chr15 affecting intron 2 of *FGF7* (Figure 3e-g). Segregation analysis revealed paternal inheritance for this *FGF7* variant (Figure 3d; Figure S2d,e,g).

3.2.3 | Family 3

Of the 3,025,718 small variants called in the WGS data of individual 3 only 17 were heterozygous, rare and of good quality with a potential truncating, splice, or loss-of-function effect (Figure 4g). This included the heterozygous variant *PITX2*(NM_000325.6):c.754_755del p.(Leu252Glufs*5) (Figure 4f). Parental segregation analysis revealed inheritance from the affected father (Figure 4e; Figure S2h–j).

3.2.4 | Family 4

No variant of interest could be identified among the small variant calls of the WGS data of individual 4. This prompted the analysis of structural variants. Of the called 21,471 structural variants only 187 were larger than 50 bp, of good quality, and rare (Figure 5f). Matching these variants to the phenotypic data of the affected loci identified the heterozygous variant *PAX9*(NM_006194.4):c.5-104_631+1087del p.? which represents a deletion of exon 3 of the *PAX9* gene (Figure 5e,g). Parental segregation analysis revealed this *PAX9* variant to have occurred de novo (Figure 5d,h; Figure S2k,l).

3.3 | Results of variant evaluation

Next, we sought to rate the pathogenicity of the identified variants of interest using the ACMG guidelines for variant classification. (Rehder et al., 2021; Richards et al., 2015; Riggs et al., 2020).

3.3.1 | *PTH1R* in individual 1

Regarding the *PTH1R*-variant identified in individual 1 only two ACMG pathogenicity criteria were met.

The detected variant substitutes the cytosine 11 bp downstream of the exon-intron boundary of exon 9 (Figure 2e,g). Checking evolutionary conservation among mammals revealed a high stability of the mutated cytosine down to marsupials (Figure 2h). Also, computational analysis of a potential effect on splicing behavior using SpliceAI (Jaganathan et al., 2019) and MMSp (Cheng et al., 2019) predicted a potential splice variant which would alter the functionally relevant heptahelical transmembrane domain of *PTH1R* (Figure 2i,g). Thus, we assigned ACMG criterion PP3-supporting. Reviewing the gnomAD database for the variant's frequency showed that it is absent from the healthy general population (Karczewski et al., 2020). Therefore, we also assigned the ACMG criterion PM2-supporting.

Since only these two criteria apply and *PTH1R* has previously only been associated with PFE and not with oligodontia, the identified *PTH1R* variant could only be classified as a variant of uncertain significance (ACMG class III).

3.3.2 | *WNT10A* and *FGF7* in individual 2

In the case of the *WNT10A* variant identified in individual 2, four ACMG pathogenicity criteria were rated positive.

WNT10A(NM_025216.3): c.321C>A p.(Cys107*) is an early nonsense mutation (Figure 3k,l) and loss of function is the known mechanism of pathogenic *WNT10A* variants (Xu et al., 2017). We, thus, assigned the ACMG criterion PVS1-very strong. Enquiring the gnomAD database for the variant's frequency in the healthy general population revealed that it is rare only amounting to 0.6% with no homozygous carriers listed in the database (Karczewski et al., 2020). Hence, we assigned the criterion PM2-supporting. Querying ClinVar and HGMD to check whether the variant's pathogenicity has previously been rated, showed that it is indeed listed as pathogenic in both databases (ClinVar ID #4461, HGMD ID #CM094234) (Bohring et al., 2009; Mostowska et al., 2013). Accordingly, we rated the criterion PP5-strong as positive. Intriguingly, the patient's phenotype of oligodontia with 10 missing permanent teeth (Figure 3a–c) perfectly fits with selective tooth agenesis type 4 associated with pathogenic *WNT10A* mutations (MIM: #150400). We, therefore, assigned the criterion PP4-supporting.

Having matched these four ACMG criteria, we rated *WNT10A*(NM_025216.3): c.321C>A p.(Cys107*) as a class V variant (pathogenic), which we consider causative for the patient's phenotype. Yet, we could not identify a second pathogenic *WNT10A* variant in individual 2.

We, however, identified an intriguing deletion in *FGF7*. Since the deletion is a (i) non-coding variant (ii) affecting a gene of unknown significance, the ACMG criteria of Richards et al. are not directly applicable. We, therefore, sought to rate the variant's significance by an approach adapted for non-coding elements from the ACMG criteria's dimensions.

Both, the WNT and FGF pathway, are important regulators of embryonic tooth development (Figure 1). As a member of the fibroblast growth factor family, *FGF7* plays a key role in the

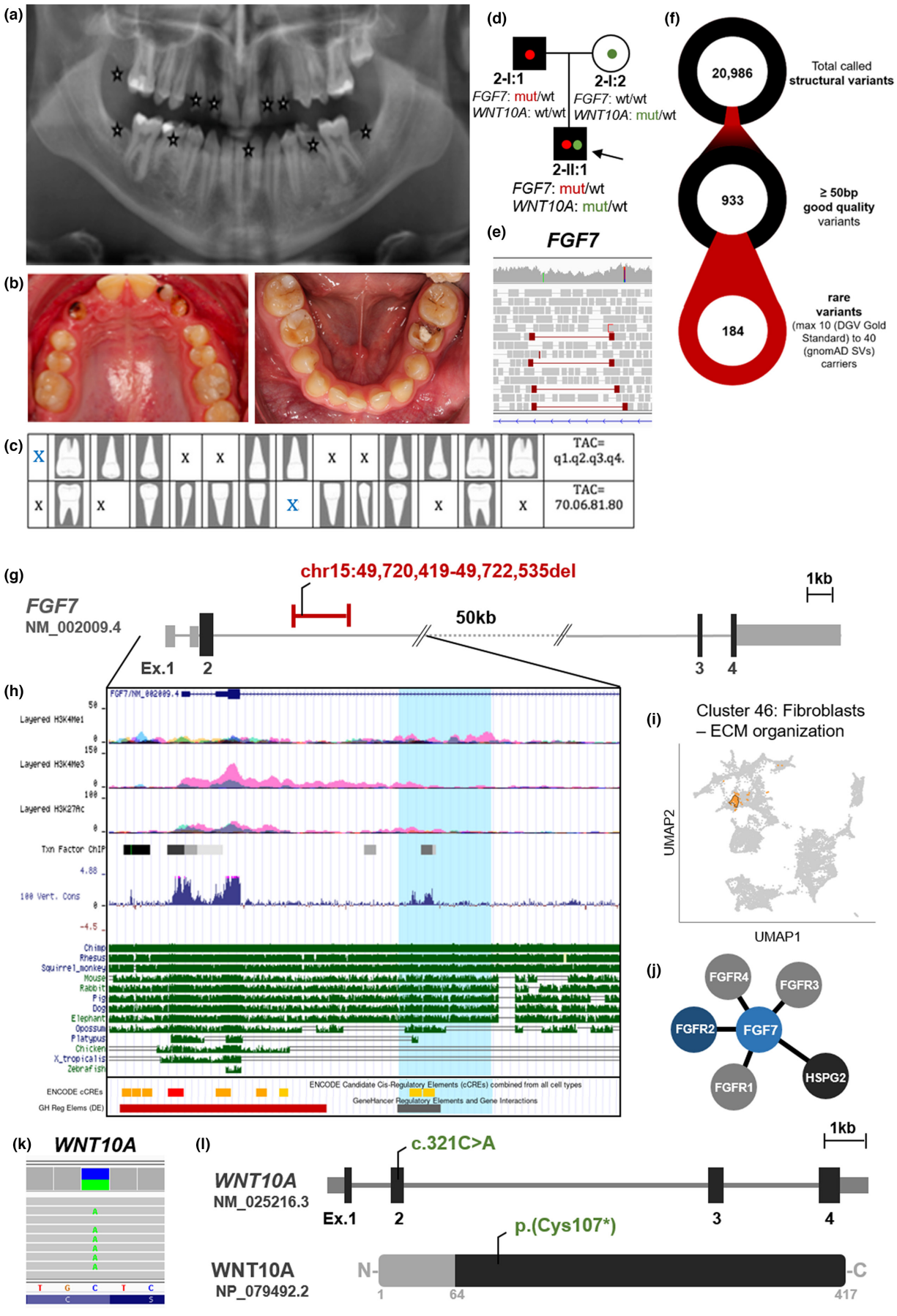

FIGURE 3 Clinical and molecular findings in individual 2: (a) Orthopantomogram shows missing teeth(*) 17,13, 12, 22, 23, 37, 35, 31, 45, 47. (b) Intraoral photographs of the index patient's maxilla and mandible show missing teeth 17,13, 12, 22, 23, 37, 35, 31, 45, 47, persistent severely decayed primary teeth 53, 62, 63, 75, 85. (c) Schematic representation of the missing teeth and coding of the phenotype with the TAC code. Asymmetric missing teeth are indicated by the blue X. (d) Pedigree: affected individuals are shown in black; mutation carriers are marked by a red (*FGF7* variant) and/or green (*WNT10A* variant) dot, arrow: index, mut: mutant allele, wt: wildtype allele, n.t.: not tested. (e) IGV screenshot of the index' NGS data showing the identified intronic *FGF7* deletion. (f) Genome SV filter strategy leading to the identified intronic *FGF7* deletion. (g) *FGF* gene. Exons (Ex.) 1–4 and the location of the identified variant are depicted. (h) Conservation across different species (blue and green) and ENCODE data (H3K4Me1, H3K4Me3, H3K27Ac, Txn Factor ChIP) of the affected position (highlighted in light blue). (i) scRNA-seq data from The Human Protein Atlas (Karlsson et al., 2021; Uhlén et al., 2015) showing *FGF7* within a cluster of Fibroblasts—ECM organization. (j) Interactors of FGF7 taken from the STRING database (Szklarczyk et al., 2021). (k) IGV screenshot of the index' NGS data showing the identified *WNT10A* variant. (l) *WNT10A* gene (above) and protein (below). Exons (Ex.) 1–4 (above, gene), functional domains (protein, below) and the location of the identified variant within these are depicted.

development of connective tissue such as cartilage, bone, and enamel (Figure 3i,j) (Pérez-Mora et al., 2023; Poudel et al., 2017; Yonei-Tamura et al., 1999). Evaluating a potential functional effect of the *FGF7* variant using the ENCODE data (ENCODE Project Consortium, 2012) shows that this intronic deletion abrogates a potential transcription factor binding site, which displays significant histone3 lysine4 monomethylation (H3K4Me1) (Figure 3h). Assessing evolutionary stability revealed that the deleted element is conserved down to platypus (Figure 3h). Reviewing the gnomAD database for the variant's frequency showed that it is absent from the healthy general population (Karczewski et al., 2020). Notably, testing the variants' inheritance showed that the *WNT10A* variant was maternally and the *FGF7* variant paternally inherited (Figure 3d). Which is in line with the hypothesis of a digenic mode of inheritance and would explain why in contrast to their son neither parent is affected by oligodontia.

Hence, we suggest the deletion in *FGF7* as a candidate for a pathogenic modifier in *WNT10A*-associated oligodontia.

3.3.3 | *PITX2* in individual 3

Applying the ACMG guidelines on the *PITX2* variant identified in individual 3 yielded four positive criteria.

In silico analysis of the frameshift's potential deleteriousness by MutationTaster (Schwarz et al., 2014) predicted it to be pathogenic and the variant features a CADD score greater than 25 (Figure S1f). The variant truncates the C-terminal 73 amino acids of PITX2, including the highly conserved OAR domain of the paired-like homeodomain transcription factor 2 (Figure 4f,i–k). This truncation equals a loss of 22% (73 of 324 amino acids) which is >10% of the protein which is loss-of-function intolerant as predicted by a pLI-score of 0.98 and a pLOEUF score of 0.26 (Figure S1e,f). Therefore, we rated the ACMG criterion PVS1-strong positive. Determining the variant's frequency using the gnomAD database revealed that *PITX2*(NM_000325.6):c.754_755del p.(Leu252Glufs*5) is absent from the healthy population (Karczewski et al., 2020). We, thus, assigned the ACMG criterion PM2-supporting. Heterozygous loss-of-function *PITX2* variants have been associated with Axenfeld-Rieger syndrome 1 (MIM:180550), a phenotype comprising certain congenital eye anomalies (anterior segment dysgenesis), umbilical, anal as well as genitourinary malformations, growth hormone deficiency, heart defects, and, notably, tooth agenesis (Semina et al., 1996; Seifi & Walter, 2018; Zhou et al., 2022; Arte et al., 2023 Jan 9). Since the father and other paternal family members were also reported to have missing teeth, both parents were tested to determine the variant's inheritance. This showed that the variant was paternally inherited (Figure 4e,h). We, therefore, assigned the ACMG criterion PP1-supporting. The phenotype of individual three matches the symptoms of Axenfeld-Rieger syndrome 1.

However, the isolated oligodontia (without ophthalmological symptoms) reported by the father would be unusual for *PITX2* mutation carriers. To further elucidate a possible association of the father's phenotype with the *PITX2* variant identified in family 3, he was ophthalmologically investigated. This revealed a posterior embryotoxon of the right eye and discrete goniosynechiae of both eyes combined with borderline intraocular pressures but without optic nerve head alterations (Figure S1c). To evaluate a possible connection between the father's phenotype and the identified *PITX2* variant, we also reviewed the literature for *PITX2*-associated phenotypes. The 51 nonsense and frameshift variants listed in the Human Gene Mutation Database (HGMD, https://apps.ingenuity.com/ingsso/login) (Stenson et al., 2014) as causative for Axenfeld-Rieger syndrome are scattered across all three of the gene's exons (Figure 4k; Table S1). Two previous pathogenic *PITX2* variants are reported to cause severe oligodontia: one with an only mild (Fan et al., 2019) and one even without an ocular phenotype (Intarak et al., 2018). Notably, the patient carrying the variant PITX2(NM_000325.6):c.630insCG p.(Val211fs) reported by Fan et al. was, nevertheless, diagnosed with Axenfeld-Rieger syndrome (Fan et al., 2019). Intriguingly, just like the variant c.754_755del p.(Leu193fs), these other two variants seen in individuals with a predominantly dental phenotype are frameshifts affecting the final (third) exon of *PITX2* (Figure 4k). Moreover, mandibular molars are less frequently missing in Axenfeld-Rieger syndrome (Figure S1g,h; Table S2) and deciduous teeth appear not to be affected. This matches the pattern of missing teeth in the father of individual 3. Given these findings, we applied the ACMG criterion PP4-strong.

In accordance with the ACMG guidelines we, thus, classified the *PITX2*-frameshift detected in family 3 as a class V variant (pathogenic).

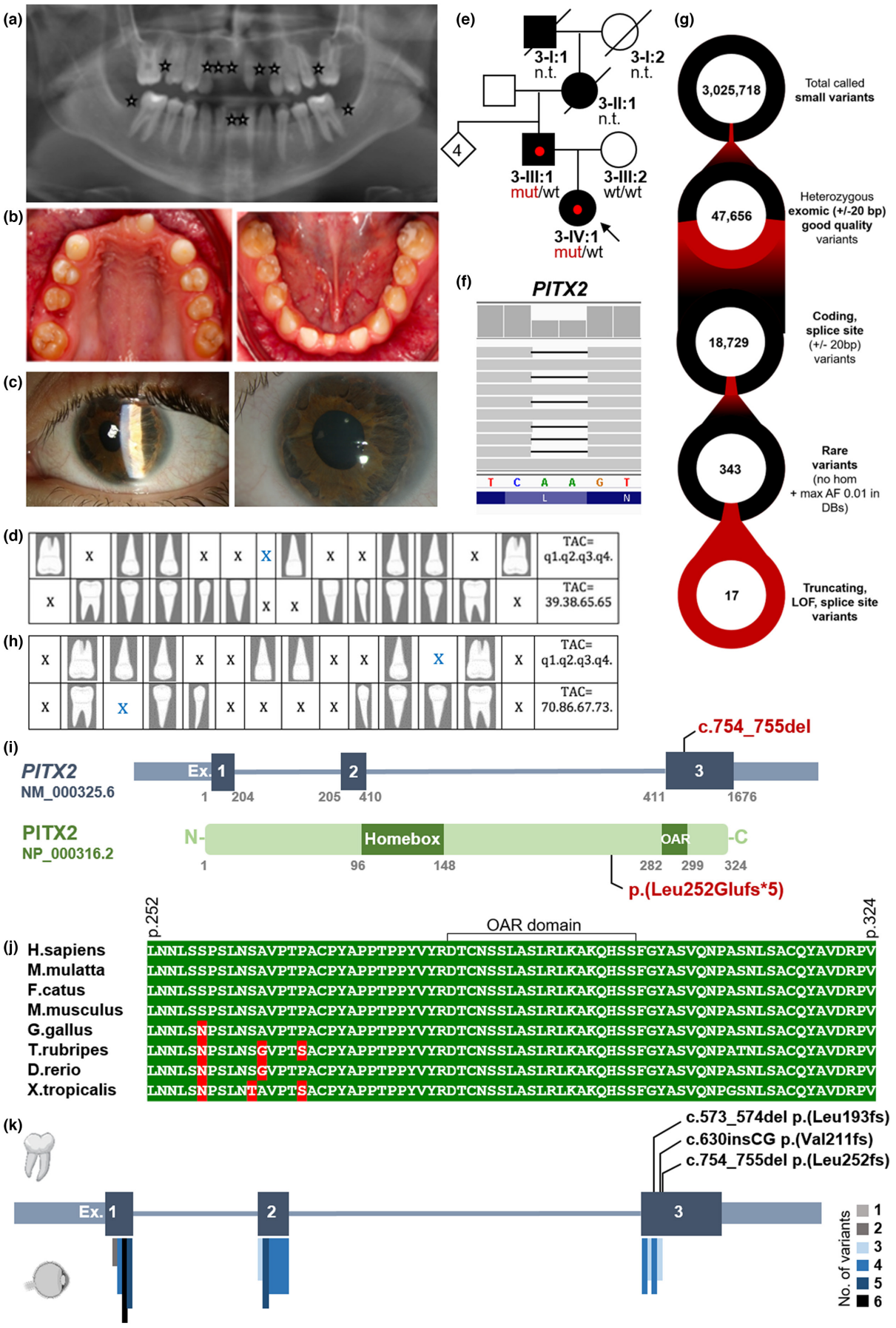

FIGURE 4 Clinical and molecular findings in individual 3: (a) Orthopantomogram of individual 3 shows missing teeth(*) 16, 13, 12, 11, 22, 23, 26, 37, 31, 41, 47 (b) Intraoral photographs of individual 3 show missing teeth 16, 13, 12, 11, 22, 23, 26, 37, 31, 41, 47, mesial migration 17, 27, microdontia 21, persistent deciduous teeth 53, 63, 81. (c) Slit lamp examination of the left eye of individual 3 shows corectopia with multiple peripheral anterior adhesions and corectopia of the left eye with multiple peripheral anterior adhesions. Photograph of the right eye shows posterior embryotoxon (d) Indexpatient: Schematic representation of the missing teeth and coding of the phenotype with the TAC code. Asymmetric missing teeth are indicated by a blue X. (e) pedigree: affected individuals are shown in black, mutation carriers are marked by a red dot, arrow: index, mut: mutant allele, wt: wildtype allele, n.t.: not tested. (f) IGV screenshot of the index' NGS data showing the identified *PITX2* variant in heterozygous state. (g) Genome SNV filter strategy leading to the identified *PITX2* variant. (h) Schematic representation of the missing teeth and coding of the phenotype with the TAC for the father of individual 3. Asymmetrically missing teeth are indicated by a blue X. (i) *PITX2* gene (above) and protein (below). Exons (Ex.) 1–3 (gene level, blue), functional domains (protein level, green) and the location of the identified variant within these are depicted. (j) Conservation of the N-terminal protein sequence of PITX2 lost due to the identified frameshift variant across different species. (k) above: *PITX2* frameshift variants reported to be associated with only mild ocular findings or even isolated oligodontia only. below: number of *PITX2* stop-gain and frameshift variants in the respective region of the *PITX2* gene causative for Axenfeld Rieger syndrome as listed in HGMD (Stenson et al., 2014).

3.3.4 | *PAX9* in individual 4

Four ACMG criteria were met regarding the *PAX9* exon 3 deletion in individual 4. Querying the deletion's frequency in the gnomAD database showed that it is absent from the healthy population (Karczewski et al., 2020). Therefore, we assigned the ACMG criterion PM2-supporting.

Pathogenic loss-of-function variants of *PAX9* are associated with selective tooth agenesis type 3 (MIM:#604635) (Fauzi et al., 2018; Stockton et al., 2000) which specifically matches the index' phenotype. Thus, we assigned the ACMG criterion PP4-strong. The deletion abrogates approximately two thirds from the N-terminus of the predicted protein sequence (i.e., >10%), including the entire functionally relevant paired box domain rendering it a loss-of-function variant. We, thus, assigned the ACMG criterion PVS1-strong. Trio-qPCR showed that the deletion arose de novo, which is in line with the index being the only family member with oligodontia (Figure 5d,h) and prompted assignment of the ACMG criterion PM6-moderate. A literature review was performed to match the patient's oligodontic phenotype to the typical pattern of teeth missing in *PAX9*-mutation carriers. 111 cases with *PAX9* variants and detailed dental reports could be identified (Table S3). Notably, in the maxilla, the probability of missing the respective tooth increases symmetrically from medial to lateral (Figure 5i). In the mandibula, however, there seem to be separate clusters with the lowest probability of a missing tooth around the canines (positions 2–4) (Figure 5j). This matches the observed pattern of tooth agenesis in our proband (Figure 5c). We, thus, assigned the ACMG criterion PP4-strong.

All ACMG classifications are summarized in Table S4.

4 | DISCUSSION

4.1 | WGS as a single genetic test strategy

Here, we describe the use of WGS in four families with oligodontia. WGS and subsequent targeted testing applied on 11 members of four families identified variants of interest in all four families. WGS identified both relevant point mutations (including coding and potential splice variants) and relevant structural deletions. Two of the pathogenic variants are novel. One case featured a variant of uncertain significance in *PTH1R*. In each of the other three cases, we identified one variant classified as pathogenic: a novel frameshift variant in *PITX2* inherited from an affected parent, a novel de novo structural variant in *PAX9*, and a nonsense variant in *WNT10A* inherited from an unaffected mother. Intriguingly, a paternally inherited non-coding potential modifier in *FGF7* was also identified in the individual featuring the maternal *WNT10A* variant. Nevertheless, more functional data and especially the identification of comparable *PTH1R* and *FGF7* variants in independent families featuring oligodontia is required for confirmation as disease loci. Deleting the putative functional element in *FGF7* in a heterozygous *Wnt10a* knockout mouse could help to further evaluate its role in oligodontia.

Notably, both the single exon deletion identified in *PAX9* and the intronic deletion found in *FGF7* were less than 2 kb in size. These would have likely been missed by microscopic chromosome analysis as well as standard resolution array comparative genomic hybridization (aCGH) (Szczałuba & Demkow, 2017). Since the breakpoints of both deletions are (deep) intronic (and thus not exomic), they would also have likely been missed by whole exome sequencing. Even trying to call the deletion in *PAX9* by a coverage drop of exon 3 would have been troublesome. This indirect approach yields a sensitivity of only 40%–80% if less than five exons are deleted, with high false-positive rates especially in single exon deletions (Kuśmirek, 2022; O'Fallon et al., 2022). Their detection, thus, usually requires other testing techniques (e.g., high-resolution aCGH, targeted fluorescence in situ hybridization (FiSH), targeted qPCR). And, not least, the immediate calling of the exact breakpoints is only possible by WGS.

Our findings add to the growing evidence suggesting that WGS could serve as a single comprehensive test in the routine diagnostic workup of patients with inborn malformations suggestive of a genetic etiology (Elsner et al., 2021; Turro et al., 2020). Although WGS identified variants of interests in all tested index patients with dental malformations, we only investigated a relatively small cohort of patients. While our data suggest that missing of more than six teeth hints to a monogenic cause evaluable by WGS, further research

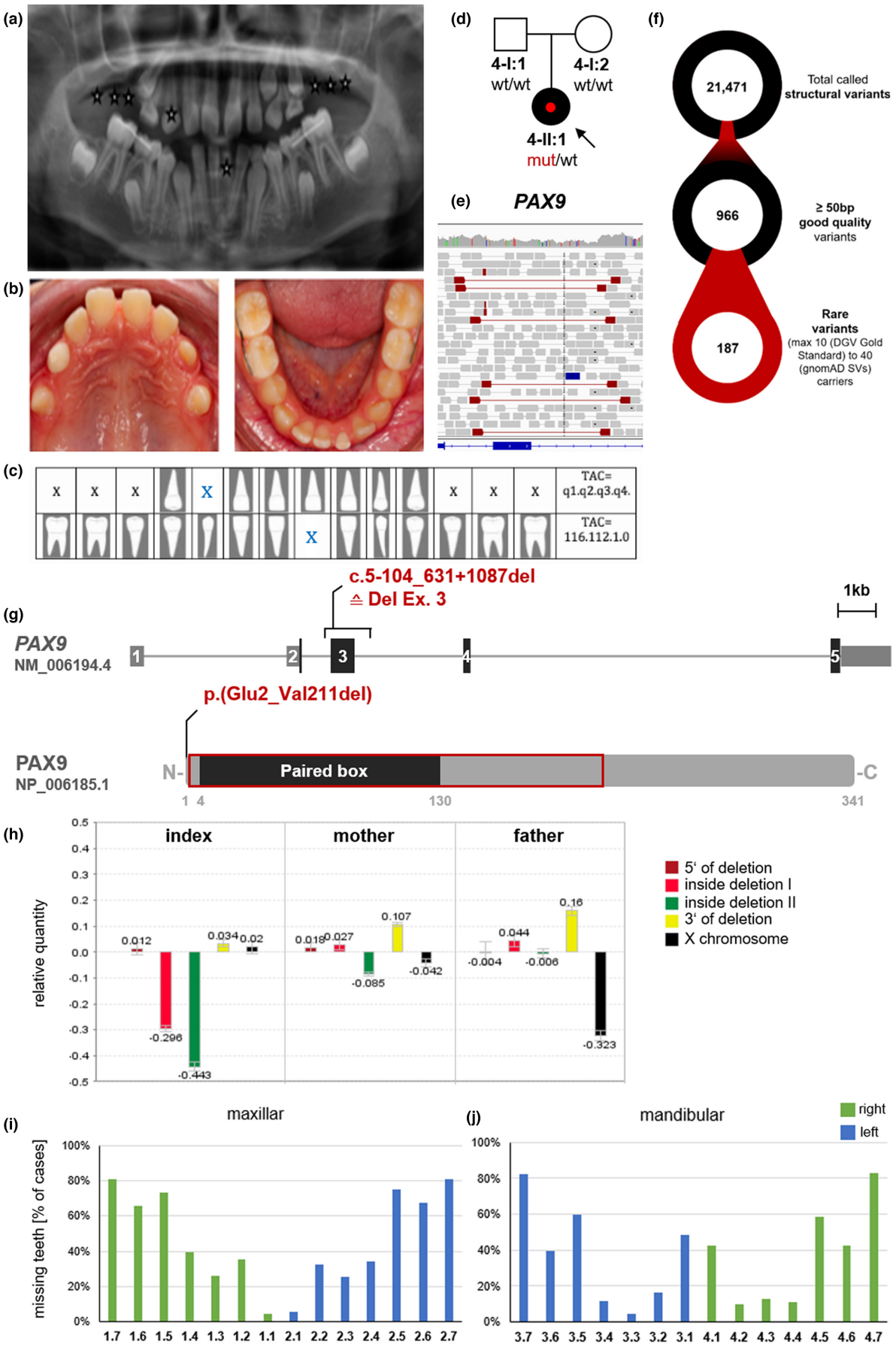

FIGURE 5 Clinical and molecular findings in individual 4: (a) Orthopantomogram shows missing teeth(*) 17, 16, 15, 13, 25, 26, 27, 31, persistent deciduous teeth 53, 54, 63, 64, 75, 73, 71, 85. (b) Discrepancies between photos and radiograms due to differing age, Intraoral photographs of the index patient's maxilla and mandible show missing teeth 17, 16, 15, 13, 25, 26, 27, 31, persistent deciduous teeth 53, 75, 71, 85, vestibular fixed retainers 75–36, and 85–46. (c) Schematic representation of the missing teeth and coding of the phenotype with the TAC. Asymmetric missing teeth are indicated by a blue X. (d) Pedigree: affected individuals are shown in black, mutation carriers are marked by a red dot, arrow: index, mut: mutant allele, wt: wildtype allele, n.t.: not tested. (e) IGV screenshot of the index' NGS data showing the identified *PAX9* deletion. (f) Genome SV filter strategy leading to the identified *PAX9* deletion. (g) *PAX9* gene (above) and protein (below). Exons (Ex.) 1–5 (gene level, above), functional domains (protein level, below) and the location of the identified deletion within these are depicted. (h) qPCR on genomic DNA of individual 4 and the parents for the identified *PAX9* deletion and neighboring regions (5′ and 3′), X chromosome as a control. (i) missing teeth in PAX9 cases from the literature: percentage of missing teeth at the respective position as determined by literature review (Table S3).

using WGS on larger cohorts of families with dental malformations is necessary to elucidate its exact potential. Such cohorts could be built by offering WGS to all patients with dental malformations. Notably, prices for WGS have plummeted in recent years with estimates being lower than 2000$ per case. Further price reductions are expected so that prices of WGS and WES will not differ strongly anymore (Schwarze et al., 2018).

4.2 | *PITX2* genotype–phenotype correlation

Moreover, our findings expand the genotypic and phenotypic spectra of *PITX2*-associated oligodontia. *PITX2* has previously only been linked to Axenfeld-Rieger syndrome type 1, a complex malformation syndrome affecting various organ systems (Arte et al., 2023; Semina et al., 1996; Seifi & Walter, 2018; Zhou et al., 2022 Jan 9). The phenotype is variable. However, the combination of functionally relevant eye anomalies (anterior segment dysgenesis) and tooth agenesis is considered pathognomonic. Hence, the phenotype featuring predominantly oligodontia and comparatively mild ocular malformations in the father of individual 3 (i.e., the accompanying visual impairment did not prompt visiting an ophthalmologist) is of particular interest.

Intriguingly, the *PITX2* variant identified in family 3 is positioned in the gene's final exon. So, too, are the two other variants described in the literature to be associated with no or only mild ophthalmologic symptoms (Fan et al., 2019; Intarak et al., 2018). Thus, they probably escape nonsense-mediated decay, only changing the C-terminal part including the OAR domain of PITX2. This sets them apart from other more upstream pathogenic *PITX2* variants, which result in a complete loss of function of the protein. *PITX2* variants can, therefore, not only cause forms of ARS1 with tooth agenesis as the leading symptom and only mild eye anomalies; but they also follow a striking genotype–phenotype correlation: the dental aspect of *PITX2*-associated disorders is mainly caused by loss of the OAR domain, while ocular and other malformations of the Axenfeld-Rieger phenotype are predominantly due to complete *PITX2* haploinsufficiency.

The association of *PITX2* with Axenfeld-Rieger syndrome also holds implications for the gene's developmental role. The formation of the primordial enamel organ requires the invagination of surface ectoderm into underlying mesenchyme. So does the embryonic development of the lens vesicle (the primordial structure of the anterior segment of the eye) (Bilodeau & Hunter, 2021; Cvekl & Camerino, 2022; Thesleff, 2014). Impairment of this process has been described in *Pitx2* conditional knockout mice (*Pitx2*^{cKO}) (Yu et al., 2020). Axenfeld-Rieger syndrome also implies the role of *PITX2* in this developmental process. Presence of a single functional *PITX2* allele appears to be sufficient for the formation of primary teeth (deciduous teeth and permanent molars) but insufficient for the budding of the dental germs (Figure 1) of the secondary teeth. Further research is needed to determine whether other genes take over the functions of *PITX2* in the embryonic development of primary teeth.

4.3 | Conclusion

In summary, WGS could be a useful diagnostic technique in individuals with a reduced number of permanent teeth. *PITX2* variants should be considered in individuals with oligodontia and no or only mild ocular findings. Regulatory elements in *FGF7* are candidates for potential modifiers of *WNT10A*-associated oligodontia.

AUTHOR CONTRIBUTIONS

SM, TB and MAM conceived the study. JM, HLS, SW and MAM examined the patients. JM, OK-N and TB evaluated patients' dental records. HLS and MAM analysed and interpreted the genetic data. JM, HLS and MAM wrote the manuscript. TB and SW reviewed and edited the manuscript. All authors gave their final approval and agree to be accountable for all aspects of the work.

ACKNOWLEDGMENTS

We thank all families for their participation. H.L.S. is a participant in the BIH Charité Junior Clinician Scientist Program and M.A.M. in the BIH Charité Digital Clinician Scientist Program founded by the late Prof. Duska Dragun and funded by the Charité—Universitätsmedizin Berlin and the Berlin Institute of Health. Open Access funding enabled and organized by Projekt DEAL.

CONFLICT OF INTEREST STATEMENT

The authors declare no conflict of interest.

DATA AVAILABILITY STATEMENT

All clinical data are submitted with the manuscript, sequencing data are available upon reasonable request.

ORCID

Theodosia Bartzela https://orcid.org/0000-0001-8478-2078

Martin A. Mensah https://orcid.org/0000-0001-8080-8779

REFERENCES

Adaimy, L., Chouery, E., Megarbane, H., Mroueh, S., Delague, V., Nicolas, E., Belguith, H., de Mazancourt, P., & Megarbane, A. (2007). Mutation in WNT10A is associated with an autosomal recessive ectodermal dysplasia: The odonto-onycho-dermal dysplasia. *American Journal of Human Genetics*, *81*(4), 821–828.

Al-Ani, A. H., Antoun, J. S., Thomson, W. M., Merriman, T. R., & Farella, M. (2017). Hypodontia: An update on its etiology, classification, and clinical management. *BioMed Research International*, *2017*, 9378325.

Arte, S., Parmanen, S., Pirinen, S., Alaluusua, S., & Nieminen, P. (2013). Candidate gene analysis of tooth agenesis identifies novel mutations in six genes and suggests significant role for WNT and EDA signaling and allele combinations. *PLoS One*, *8*(8), e73705.

Arte, S., Pöyhönen, M., Myllymäki, E., Ronkainen, E., Rice, D. P., & Nieminen, P. (2023). Craniofacial and dental features of Axenfeld-Rieger syndrome patients with PITX2 mutations. *Orthodontics & Craniofacial Research*, *26*, 320–330. https://doi.org/10.1111/ocr.12631

Bailleul-Forestier, I., Molla, M., Verloes, A., & Berdal, A. (2008). The genetic basis of inherited anomalies of the teeth. Part 1: Clinical and molecular aspects of non-syndromic dental disorders. *European Journal of Medical Genetics*, *51*(4), 273–291.

Biedziak, B., Firlej, E., Dąbrowska, J., Bogdanowicz, A., Zadurska, M., & Mostowska, A. (2022). Novel candidate genes for non-syndromic tooth agenesis identified using targeted next-generation sequencing. *Journal of Clinical Medical Research*, *11*(20), 6089. https://doi.org/10.3390/jcm11206089

Bilodeau, E. A., & Hunter, K. D. (2021). Odontogenic and developmental Oral lesions in pediatric patients. *Head and Neck Pathology*, *15*(1), 71–84.

Bohring, A., Stamm, T., Spaich, C., Haase, C., Spree, K., Hehr, U., Hoffmann, M., Ledig, S., Sel, S., Wieacker, P., & Röpke, A. (2009). WNT10A mutations are a frequent cause of a broad spectrum of ectodermal dysplasias with sex-biased manifestation pattern in heterozygotes. *American Journal of Human Genetics*, *85*(1), 97–105.

Cheng, J., Nguyen, T. Y. D., Cygan, K. J., Çelik, M. H., Fairbrother, W. G., Avsec, Ž., & Gagneur, J. (2019). MMSplice: Modular modeling improves the predictions of genetic variant effects on splicing. *Genome Biology*, *20*(1), 48.

Cobourne, M. T., & Sharpe, P. T. (2013). Diseases of the tooth: The genetic and molecular basis of inherited anomalies affecting the dentition. *Wiley Interdisciplinary Reviews: Developmental Biology*, *2*(2), 183–212.

Cvekl, A., & Camerino, M. J. (2022). Generation of lens progenitor cells and lentoid bodies from pluripotent stem cells: Novel tools for human lens development and ocular disease etiology. *Cell*, *11*(21), 3516. https://doi.org/10.3390/cells11213516

de La Dure-Molla, M., Fournier, B. P., Manzanares, M. C., Acevedo, A. C., Hennekam, R. C., Friedlander, L., Boy-Lefèvre, M.-L., Kerner, S., Toupenay, S., Garrec, P., & Vi-Fane, B. (2019). Elements of morphology: Standard terminology for the teeth and classifying genetic dental disorders. *American Journal of Medical Genetics. Part A*, *179*(10), 1913–1981.

Decker, E., Stellzig-Eisenhauer, A., Fiebig, B. S., Rau, C., Kress, W., Saar, K., Rüschendorf, F., Hubner, N., Grimm, T., & Weber, B. H. F. (2008). PTHR1 loss-of-function mutations in familial, nonsyndromic primary failure of tooth eruption. *American Journal of Human Genetics*, *83*(6), 781–786.

Elsner, J., Mensah, M. A., Holtgrewe, M., Hertzberg, J., Bigoni, S., Busche, A., Coutelier, M., de Silva, D. C., Elçioglu, N., Filges, I., Gerkes, E., Girisha, K. M., Graul-Neumann, L., Jamsheer, A., Krawitz, P., Kurth, I., Markus, S., Megarbane, A., Reis, A., … Spielmann, M. (2021). Genome sequencing in families with congenital limb malformations. *Human Genetics*, *140*(8), 1229–1239.

ENCODE Project Consortium. (2012). An integrated encyclopedia of DNA elements in the human genome. *Nature*, *489*(7414), 57–74.

ENCODE Project Consortium, Moore, J. E., Purcaro, M. J., Pratt, H. E., Epstein, C. B., Shoresh, N., Adrian, J., Kawli, T., Davis, C. A., Dobin, A., & Kaul, R. (2020). Expanded encyclopaedias of DNA elements in the human and mouse genomes. *Nature*, *583*(7818), 699–710.

Fan, Z., Sun, S., Liu, H., Yu, M., Liu, Z., Wong, S.-W., Liu, Y., Han, D., & Feng, H. (2019). Novel PITX2 mutations identified in Axenfeld-Rieger syndrome and the pattern of PITX2-related tooth agenesis. *Oral Diseases*, *25*(8), 2010–2019.

Fauzi, N. H., Ardini, Y. D., Zainuddin, Z., & Lestari, W. (2018). A review on non-syndromic tooth agenesis associated with mutations. *Japanese Dental Science Review*, *54*(1), 30–36.

Fishilevich, S., Nudel, R., Rappaport, N., Hadar, R., Plaschkes, I., Iny Stein, T., Rosen, N., Kohn, A., Twik, M., Safran, M., & Lancet, D. (2017). *GeneHancer: Genome-wide integration of enhancers and target genes* In GeneCards Database. 2017. https://doi.org/10.1093/database/bax028

Holtgrewe, M., Stolpe, O., Nieminen, M., Mundlos, S., Knaus, A., Kornak, U., Seelow, D., Segebrecht, L., Spielmann, M., Fischer-Zirnsak, B., Boschann, F., Scholl, U., Ehmke, N., & Beule, D. (2020). VarFish: Comprehensive DNA variant analysis for diagnostics and research. *Nucleic Acids Research*, *48*(W1), W162–W169.

Intarak, N., Theerapanon, T., Ittiwut, C., Suphapeetiporn, K., Porntaveetus, T., & Shotelersuk, V. (2018). A novel PITX2 mutation in non-syndromic orodental anomalies. *Oral Diseases*, *24*(4), 611–618.

Ioannidis, N. M., Rothstein, J. H., Pejaver, V., Middha, S., McDonnell, S. K., Baheti, S., Musolf, A., Li, Q., Holzinger, E., Karyadi, D., & Cannon-Albright, L. A. (2016). REVEL: An ensemble method for predicting the pathogenicity of rare missense variants. *American Journal of Human Genetics*, *99*(4), 877–885.

Jaganathan, K., Kyriazopoulou Panagiotopoulou, S., McRae, J. F., Darbandi, S. F., Knowles, D., Li, Y. I., Kosmicki, J. A., Arbelaez, J., Cui, W., Schwartz, G. B., & Chow, E. D. (2019). Predicting splicing from primary sequence with deep learning. *Cell*, *176*(3), 535–548.e24.

Karczewski, K. J., Francioli, L. C., Tiao, G., Cummings, B. B., Alföldi, J., Wang, Q., Collins, R. L., Laricchia, K. M., Ganna, A., Birnbaum, D. P., Gauthier, L. D., Brand, H., Solomonson, M., Watts, N. A., Rhodes, D., Singer-Berk, M., England, E. M., Seaby, E. G., Kosmicki, J. A., … MacArthur, D. G. (2020). The mutational constraint spectrum quantified from variation in 141,456 humans. *Nature*, *581*(7809), 434–443.

Karlsson, M., Zhang, C., Méar, L., Zhong, W., Digre, A., Katona, B., Sjöstedt, E., Butler, L., Odeberg, J., Dusart, P., Edfors, F., Oksvold, P., von Feilitzen, K., Zwahlen, M., Arif, M., Altay, O., Li, X., Ozcan, M., Mardinoglu, A., … Lindskog, C. (2021). A single-cell type transcriptomics map of human tissues. *Science Advances*, *7*(31), eabh2169. https://doi.org/10.1126/sciadv.abh2169

Kent, W. J., Sugnet, C. W., Furey, T. S., Roskin, K. M., Pringle, T. H., Zahler, A. M., & Haussler, D. (2002). The human genome browser at UCSC. *Genome Research*, *12*(6), 996–1006.

Kuśmirek, W. (2022). Different strategies for counting the depth of coverage in copy number variation calling tools. *Bioinformatics and Biology Insights*, *16*, 11779322221115534.

Massink, M. P. G., Créton, M. A., Spanevello, F., Fennis, W. M. M., Cune, M. S., Savelberg, S. M. C., Nijman, I. J., Maurice, M. M., van den Boogaard, M.-J. H., & van Haaften, G. (2015). Loss-of-function

mutations in the WNT Co-receptor LRP6 cause autosomal-dominant oligodontia. *American Journal of Human Genetics*, *97*(4), 621–626.

Matalova, E., Fleischmannova, J., Sharpe, P. T., & Tucker, A. S. (2008). Tooth agenesis: From molecular genetics to molecular dentistry. *Journal of Dental Research*, *87*(7), 617–623.

Mostowska, A., Biedziak, B., Zadurska, M., Dunin-Wilczynska, I., Lianeri, M., & Jagodzinski, P. P. (2013). Nucleotide variants of genes encoding components of the Wnt signalling pathway and the risk of non-syndromic tooth agenesis. *Clinical Genetics*, *84*(5), 429–440.

Murakami, A., Yasuhira, S., Mayama, H., Miura, H., Maesawa, C., & Satoh, K. (2017). Characterization of PAX9 variant P20L identified in a Japanese family with tooth agenesis. *PLoS One*, *12*(10), e0186260. https://doi.org/10.1371/journal.pone.0186260

Nieminen, M., Stolpe, O., Schumann, F., Holtgrewe, M., & Beule, D. (2020). SODAR Core: A Django-based framework for scientific data management and analysis web apps. *The Journal of Open Source Software*, *JOSS.*, *55*(5), 1584.

O'Fallon, B., Durtschi, J., Kellogg, A., Lewis, T., Close, D., & Best, H. (2022). Algorithmic improvements for discovery of germline copy number variants in next-generation sequencing data. *BMC Bioinformatics*, *23*(1), 285.

Pérez-Mora, S., Ocampo-López, J., Gómez-García, M. D. C., & Pérez-Ishiwara, D. G. (2023). BFNB enhances hair growth in C57BL/6 mice through the induction of EGF and FGF7 factors and the PI3K-AKT-β-catenin pathway. *International Journal of Molecular Sciences*, *24*(15), 12110. https://doi.org/10.3390/ijms241512110

Poudel, S. B., Bhattarai, G., Kim, J.-H., Kook, S.-H., Seo, Y.-K., Jeon, Y.-M., & Lee, J.-C. (2017). Local delivery of recombinant human FGF7 enhances bone formation in rat mandible defects. *Journal of Bone and Mineral Metabolism*, *35*(5), 485–496.

Rehder, C., Bean, L. J. H., Bick, D., Chao, E., Chung, W., Das, S., O'Daniel, J., Rehm, H., Shashi, V., Vincent, L. M., & ACMG Laboratory Quality Assurance Committee. (2021). Next-generation sequencing for constitutional variants in the clinical laboratory, 2021 revision: A technical standard of the American College of Medical Genetics and Genomics (ACMG). *Genetics in Medicine*, *23*(8), 1399–1415.

Rentzsch, P., Schubach, M., Shendure, J., & Kircher, M. (2021). CADD-splice-improving genome-wide variant effect prediction using deep learning-derived splice scores. *Genome Medicine*, *13*(1), 31.

Richards, S., Aziz, N., Bale, S., Bick, D., Das, S., Gastier-Foster, J., Grody, W. W., Hegde, M., Lyon, E., Spector, E., & Voelkerding, K. (2015). Standards and guidelines for the interpretation of sequence variants: A joint consensus recommendation of the American College of Medical Genetics and Genomics and the Association for Molecular Pathology. *Genetics in Medicine*, *17*(5), 405–424.

Riggs, E. R., Andersen, E. F., Cherry, A. M., Kantarci, S., Kearney, H., Patel, A., Raca, G., Ritter, D. I., South, S. T., Thorland, E. C., Pineda-Alvarez, D., Aradhya, S., & Martin, C. L. (2020). Technical standards for the interpretation and reporting of constitutional copy-number variants: A joint consensus recommendation of the American College of Medical Genetics and Genomics (ACMG) and the clinical genome resource (ClinGen). *Genetics in Medicine*, *22*(2), 245–257.

Schwarz, J. M., Cooper, D. N., Schuelke, M., & Seelow, D. (2014). MutationTaster2: Mutation prediction for the deep-sequencing age. *Nature Methods*, *11*(4), 361–362.

Schwarze, K., Buchanan, J., Taylor, J. C., & Wordsworth, S. (2018). Are whole-exome and whole-genome sequencing approaches cost-effective? A systematic review of the literature. *Genetics in Medicine*, *20*(10), 1122–1130.

Seifi, M., & Walter, M. A. (2018). Axenfeld-Rieger syndrome. *Clinical Genetics*, *93*(6), 1123–1130.

Semina, E. V., Reiter, R., Leysens, N. J., Alward, W. L., Small, K. W., Datson, N. A., Siegel-Bartelt, J., Bierke-Nelson, D., Bitoun, P., Zabel, B. U., & Carey, J. C. (1996). Cloning and characterization of a novel bicoid-related homeobox transcription factor gene, RIEG, involved in Rieger syndrome. *Nature Genetics*, *14*(4), 392–399.

Song, S., Han, D., Qu, H., Gong, Y., Wu, H., Zhang, X., Zhong, N., & Feng, H. (2009). EDA gene mutations underlie non-syndromic oligodontia. *Journal of Dental Research*, *88*(2), 126–131.

Stenson, P. D., Mort, M., Ball, E. V., Shaw, K., Phillips, A., & Cooper, D. N. (2014). The human gene mutation database: Building a comprehensive mutation repository for clinical and molecular genetics, diagnostic testing and personalized genomic medicine. *Human Genetics*, *133*(1), 1–9.

Stockton, D. W., Das, P., Goldenberg, M., D'Souza, R. N., & Patel, P. I. (2000). Mutation of PAX9 is associated with oligodontia. *Nature Genetics*, *24*(1), 18–19.

Szczałuba, K., & Demkow, U. (2017). Array comparative genomic hybridization and genomic sequencing in the diagnostics of the causes of congenital anomalies. *Journal of Applied Genetics*, *58*(2), 185–198.

Szklarczyk, D., Gable, A. L., Nastou, K. C., Lyon, D., Kirsch, R., Pyysalo, S., Doncheva, N. T., Legeay, M., Fang, T., Bork, P., Jensen, L. J., & von Mering, C. (2021). The STRING database in 2021: Customizable protein-protein networks, and functional characterization of user-uploaded gene/measurement sets. *Nucleic Acids Research*, *49*(D1), D605–D612.

Thesleff, I. (2014). Current understanding of the process of tooth formation: Transfer from the laboratory to the clinic. *Australian Dental Journal.*, *59*, 48–54. https://doi.org/10.1111/adj.12102

Turro, E., Astle, W. J., Megy, K., Gräf, S., Greene, D., Shamardina, O., Allen, H. L., Sanchis-Juan, A., Frontini, M., Thys, C., Stephens, J., Mapeta, R., Burren, O. S., Downes, K., Haimel, M., Tuna, S., Deevi, S. V. V., Aitman, T. J., Bennett, D. L., … Ouwehand, W. H. (2020). Whole-genome sequencing of patients with rare diseases in a national health system. *Nature*, *583*(7814), 96–102.

Uhlén, M., Fagerberg, L., Hallström, B. M., Lindskog, C., Oksvold, P., Mardinoglu, A., Sivertsson, Å., Kampf, C., Sjöstedt, E., Asplund, A., Olsson, I. M., Edlund, K., Lundberg, E., Navani, S., Szigyarto, C. A. K., Odeberg, J., Djureinovic, D., Takanen, J. O., Hober, S., … Pontén, F. (2015). Proteomics. Tissue-based map of the human proteome. *Science*, *347*(6220), 1260419.

van Wijk, A. J., & Tan, S. P. K. (2006). A numeric code for identifying patterns of human tooth agenesis: A new approach. *European Journal of Oral Sciences*, *114*(2), 97–101.

Williams, M. A., & Letra, A. (2018). The changing landscape in the genetic etiology of human tooth agenesis. *Genes*, *9*(5), 255. https://doi.org/10.3390/genes9050255

Wong, S., Liu, H., Bai, B., Chang, H., Zhao, H., Wang, Y., Han, D., & Feng, H. (2014). Novel missense mutations in the AXIN2 gene associated with non-syndromic oligodontia. *Archives of Oral Biology*, *59*(3), 349–353.

Xu, M., Horrell, J., Snitow, M., Cui, J., Gochnauer, H., Syrett, C. M., Kallish, S., Seykora, J. T., Liu, F., Gaillard, D., Katz, J. P., Kaestner, K. H., Levin, B., Mansfield, C., Douglas, J. E., Cowart, B. J., Tordoff, M., Liu, F., Zhu, X., … Millar, S. E. (2017). WNT10A mutation causes ectodermal dysplasia by impairing progenitor cell proliferation and KLF4-mediated differentiation. *Nature Communications*, *8*, 15397.

Yonei-Tamura, S., Endo, T., Yajima, H., Ohuchi, H., Ide, H., & Tamura, K. (1999). FGF7 and FGF10 directly induce the apical ectodermal ridge in chick embryos. *Developmental Biology*, *211*(1), 133–143.

Yu, M., Liu, Y., Liu, H., Wong, S.-W., He, H., Zhang, X., Wang, Y., Han, D., & Feng, H. (2019). Distinct impacts of bi-allelic WNT10A mutations on the permanent and primary dentitions in odonto-onycho-dermal dysplasia. *American Journal of Medical Genetics. Part A*, *179*(1), 57–64.

Yu, W., Sun, Z., Sweat, Y., Sweat, M., Venugopalan, S. R., Eliason, S., Cao, H., Paine, M. L., & Amendt, B. A. (2020). Pitx2-Sox2-Lef1 interactions specify progenitor oral/dental epithelial cell signaling centers. *Development*, *147*(11), dev186023. https://doi.org/10.1242/dev.186023

Zheng, J., Yu, M., Liu, H., Cai, T., Feng, H., Liu, Y., & Han, D. (2021). Novel MSX1 variants identified in families with nonsyndromic oligodontia. *International Journal of Oral Science*, *13*(1), 2.

Zhou, L., Wang, X., An, J., Zhang, Y., He, M., & Tang, L. (2022). Genotype-phenotype association of PITX2 and FOXC1 in Axenfeld-Rieger syndrome. *Experimental Eye Research*, *226*, 109307.

SUPPORTING INFORMATION

Additional supporting information can be found online in the Supporting Information section at the end of this article.

How to cite this article: Mitscherling, J., Sczakiel, H. L., Kiskemper-Nestorjuk, O., Winterhalter, S., Mundlos, S., Bartzela, T., & Mensah, M. A. (2023). Whole genome sequencing in families with oligodontia. *Oral Diseases*, *00*, 1–16. https://doi.org/10.1111/odi.14816